

Hygrothermal Simulation of Prefabricated Cold-Formed Wall Panels

Ayman R. Hamdallah Filip Fedorik Antti H. Niemi

Civil Engineering Research Unit, University of Oulu, Finland,
{ayman.hamdallah, filip.fedorik, antti.niemi}@oulu.fi

Abstract

Steel structures are light and durable, but in the building envelope they can transfer heat energy easily from the building interior to outside and hinder the energy performance of the building. In this study, we simulate the thermal performance of cold-formed steel panels that can be used as prefabricated units in building envelopes. More precisely, the thermal performance of hollow cold-formed steel elements filled with thermal insulation is studied with varying panel geometry. The focus is on stainless steel but also mild steel is briefly considered. Attention is paid especially to the thermal bridges associated to the relatively high thermal conductivity of steel materials. The influence of the width, depth and the height of the panel to thermal bridging is assessed and panel geometries with reasonable thermal performance are found. By considering also the moisture transport, the overall hygrothermal performance of the panels is then evaluated.

Keywords: cold-formed steel, hygrothermal simulation, thermal bridge, stainless steel, prefabricated elements

1 Introduction

Cold-Formed Steel (CFS) cross-sections are used extensively in the construction industry as secondary load-carrying members, such as roof purlins and girts in framed walls. These sections are manufactured by bending flat sheets with thickness ranging typically from 0.4 mm to 6.4 mm in Europe and North America (Dubina et al., 2012; Hancock et al., 2001). Nowadays, CFS sections are employed increasingly also as primary structural elements in framing systems of single-story industrial buildings with short to intermediate spans.

Use of prefabricated wall panels provides an answer to environmental and economic demands of sustainability and quality by reducing mis-fabrication and time consumption on building sites particularly regarding the thermal insulation process in cold and humid as well as in hot and moist weather conditions. Thin cold-formed steel sheets are suitable for this purpose because they can be formed in the shape of hollow sections and transported relatively easily. When compared with traditional construction materials such as timber, or ordinary steel frames, which use mineral wool as insulation material, the cold-formed panels offer distinct benefits in construction pro-

cess, quality control, cost-effectiveness as well and sustainability.

However, the high thermal conductivity of steel means that the heat flow must be carefully controlled with insulation and that attention must be paid to thermal bridges, i.e. areas where the heat flow is locally increased. If not controlled properly, the thermal bridges may lead to higher energy costs, moisture problems and thermal discomfort of the building occupants.

The earlier study by Soares et al. reviews the main features of steel-framed construction from the point of view of life cycle energy consumption (Soares et al., 2017). The overview indicates some strategies for reducing thermal bridges and improving the thermal resistance of steel structures in the building envelope. Furthermore, the effectiveness of insulation with respect to its position in the steel-framed wall with CFS elements and non-structural panels has been recently discussed in (Roque and Santos, 2017; Roque et al., 2020; Kapoor and Peterman, 2021). By comparing CFS framing and hybrid-frame construction, the authors have observed that the location of the insulation significantly affects thermal bridges and the overall thermal performance of the wall.

Hollow tubes and other shapes can be used as structural elements in lightweight steel frames. Our study is focused on prefabricated hollow CFS wall panels that

- can be easily insulated thermally and acoustically due to the core space inside
- are easily recyclable
- have high mechanical strength combined with light weight
- reduce the risk of moisture problems because of dry construction environment
- can be transported economically
- are easy and fast to assemble

We present a family of such panels where the geometry is varied parametrically and evaluate the thermal and hygrothermal performance of the building constructions in northern conditions. It should be noted that due to their large slenderness, i.e. width-to-thickness ratio, such elements are inherently susceptible to local, distortional and

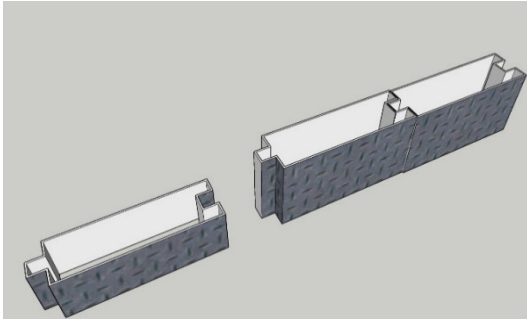


Figure 1. 3D sketch of the hollow CFS unit.

global buckling phenomena. We do not consider the structural integrity in this study but the insulation is expected to help to prevent local buckling.

The structure of the paper is as follows. The proposed wall element is introduced in the next section. Section 3 describes the models and the numerical simulation used to analyze and optimize the thermal performance of the wall element and contains the main results of the paper. Moisture transport is then considered in Section 4 and the paper ends with conclusions and remarks in Section 5.

2 Proposed Wall Element

The prefabricated wall element that we propose and analyze consists of a hollow cold-formed section filled with insulation as shown in Figure 1. Such prefabricated panels can be easily assembled at the construction site, and they form the main core of wall. This concept could be used to substitute traditional construction techniques in heated and non-heated buildings like the one shown in Figure 2. The final assembly of such wall elements shall then include e.g. a gypsum board and a suitable weather protection or cladding on the inner and outer face of the core wall respectively as shown in Figure 3.

Based on the practical demands and dimensional recommendations of the cold-formed steel industry, we choose six different panel geometries for comparison by simulation. The interior gypsum board and the weather protection layer remain unchanged as they do not contribute significantly to the overall assessment of the wall element. The studied wall elements are labeled based on



Figure 2. Storage building in Oulu, Finland.

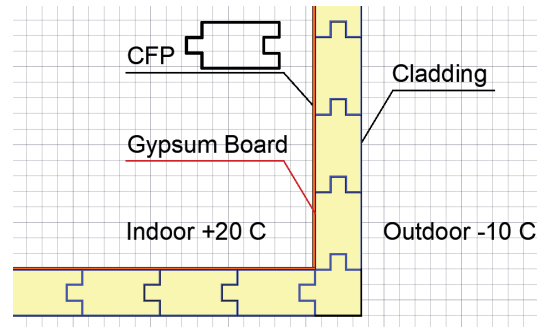


Figure 3. Conceptual model of the corner of the building made of CFS units and temperature boundary conditions.

their characteristic geometric information (width, depth, and thickness) and are listed in Table 1.

Table 1. Geometric parameters of the wall assemblies.

<i>Label</i>	<i>Width</i> [cm]	<i>Depth</i> [cm]	<i>Thickness</i> [cm]
W100-30-0.1	100	30	0.1
W100-30-0.2	100	30	0.2
W100-30-0.3	100	30	0.3
W100-15-0.2	100	15	0.2
W050-30-0.1	50	30	0.2
W150-30-0.1	150	30	0.2

Assuming a density of 7500 kg/m³ for steel and a density of 30 kg/m³ for the insulation, the unit masses of the different assemblies per square meter of building envelope are shown in Table 2 to demonstrate their practicality.

Table 2. Unit masses of the wall assemblies.

<i>Label</i>	<i>Unit Mass</i> [kg/m ²]
W100-30-0.1	39
W100-30-0.2	58.4
W100-30-0.3	77.8
W100-15-0.2	44.2
W050-30-0.1	67.4
W150-30-0.1	55.4

3 Heat Transfer Analysis

The thermal analysis is based on a steady-state heat transfer simulation of the selected wall assemblies using the COMSOL software. The basic model takes into account only heat conduction so that the governing partial differential equation is elliptic. Then the finite element method produces the best approximation of the exact temperature distribution on a given mesh. Two-dimensional models of the wall assembly were created near a rectangular corner which is the critical area concerning heat transfer in buildings and the finite element mesh was refined enough so

that the thin structural components of the assembly can be analyzed.

The main quantity of interest and optimization criterion in the thermal analysis is the linear thermal transmittance [$W/(m^2K)$] defined typically in the building codes as

$$\psi = L_{2D} - \sum_j U_j \cdot l_j, \quad (1)$$

where U_j is the thermal transmittance [$W/(m^2K)$], l_j is the length [m] over which U_j applies and L_{2D} is the thermal coupling coefficient [$W/(m^2K)$].

In our study, the thermal coupling coefficient L_{2D} is obtained by integrating the heat flow rate obtained from the numerical simulation over the interior surface including the corner and the thermal transmittances U_1 and U_2 are determined similarly as the average heat flow rate of the straight periodic wall segments. Because of symmetry, $U_1 = U_2 = U$ in our case.

3.1 Material Properties and Boundary Conditions

One of the key elements in the present analysis is the thermal transmittance due to the relatively high thermal conductivity of steel. However, there is a considerable difference between the thermal conductivities of stainless and mild steels. We use the value 15 $W/(mK)$ for stainless steel and the value 50 $W/(mK)$ for mild steel.

The thermal conductivities of the gypsum board and the weather protection layer are taken as 0.21 $W/(mK)$ and 0.06 $W/(mK)$, respectively. Furthermore, the convective heat flux boundary conditions are used on the external and internal sides of the wall by taking 1/0.04 and 1/0.13 as the external and internal heat transfer coefficients, respectively (Hopkin et al., 2011).

3.2 Results

Figure 4 shows as an example the steady-state temperature distribution and the finite element mesh for the assembly W100-30-0.2 with stainless steel. The thermal bridges at the corner as well as near the junction of two neighboring steel sections lead to slightly cooler temperatures at the interior surface of the wall.

As expected, the temperature distribution is influenced by the steel elements that have a very high thermal conductivity as compared with the insulation. The phenomenon becomes even more clear, if we look at the distribution of the heat flow rate over the interior surface of the wall assembly. Figure 5 shows the heat flow rates calculated along the interior wall surface for the wall assemblies W100-30-0.1, W150-30-0.2, and W100-15-0.2, respectively. The geometry affects somewhat significantly the heat flow rate near the corner as well as its overall distribution along the wall assembly.

The different wall element geometries are then compared in Table 3 in terms of their U -value and the thermal transmittance ψ at the corner according to Equation (1). The comparison of the assemblies shows that increasing

Table 3. Comparison of thermal characteristics of different wall assemblies.

<i>Label</i>	U [W/m^2]	ψ [$W/(mK)$]
W100-30-0.1	0.18	0.03
W100-30-0.2	0.21	0.09
W100-30-0.3	0.26	0.06
W100-15-0.2	0.39	0.05
W050-30-0.2	0.30	0.03
W150-30-0.2	0.19	0.01

the thickness of the steel sheet strengthens the thermal bridges between neighboring elements and hence the average U -value of the wall. Increasing the width of the wall unit reduces the U -value but it cannot be increased excessively because of practical reasons regarding economy and transport. On the other hand, the relationship between the geometric parameters and the thermal admittance at the corner is more complex and the performance assessment requires engineering judgement.

The influence of the specific steel type to the overall thermal characteristics of the wall assembly is addressed in Table 4 showing the thermal characteristics of the panel W100-30-0.1 made of mild steel with thermal conductivity 50 $W/(mK)$. Comparing these values with the first line of Table 3 shows that the higher thermal conductivity is reflected in the average U -value of the wall assembly and especially in the thermal bridge at the corner.

Table 4. Thermal characteristics of a wall assembly made of mild steel.

<i>Label</i>	U [W/m^2]	ψ [$W/(mk)$]
W100-30-0.1 (mild)	0.26	0.13

4 Hygrothermal Analysis

A time-dependent heat and moisture transport simulation of the wall assembly was carried out again by the COMSOL software. The outdoor boundary conditions for the temperature and the relative humidity were taken from the values recorded by the Finnish Meteorological Institute in Oulu, Finland for the year 2020. Indoor conditions were represented by temperature and relative humidity derived from the outdoor conditions according to the guidelines by the Finnish Association of Civil Engineers (Suomen Rakennusinsinöörien Liitto RIL ry, 2012). The simulation was performed for a period of two years by replicating the same boundary condition data. The reason for this is to neglect any impact of the initial conditions on the obtained results. Material properties required for coupled heat and moisture transfer analysis are thermal conductivity, heat

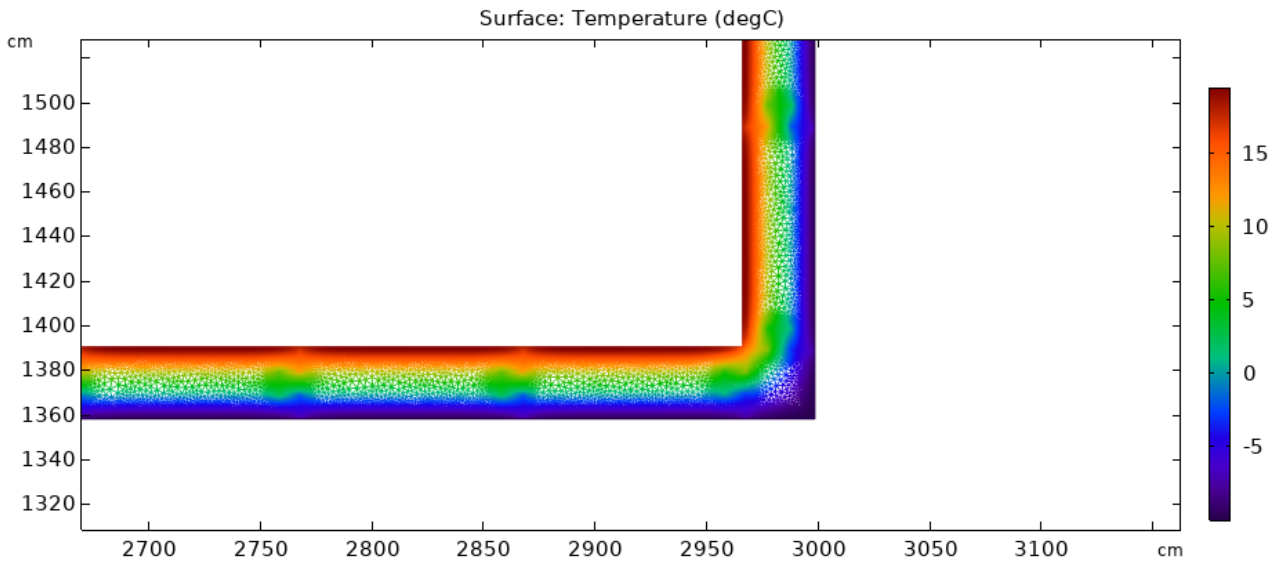


Figure 4. Temperature distribution for the assembly W100-30-0.2 with stainless steel.

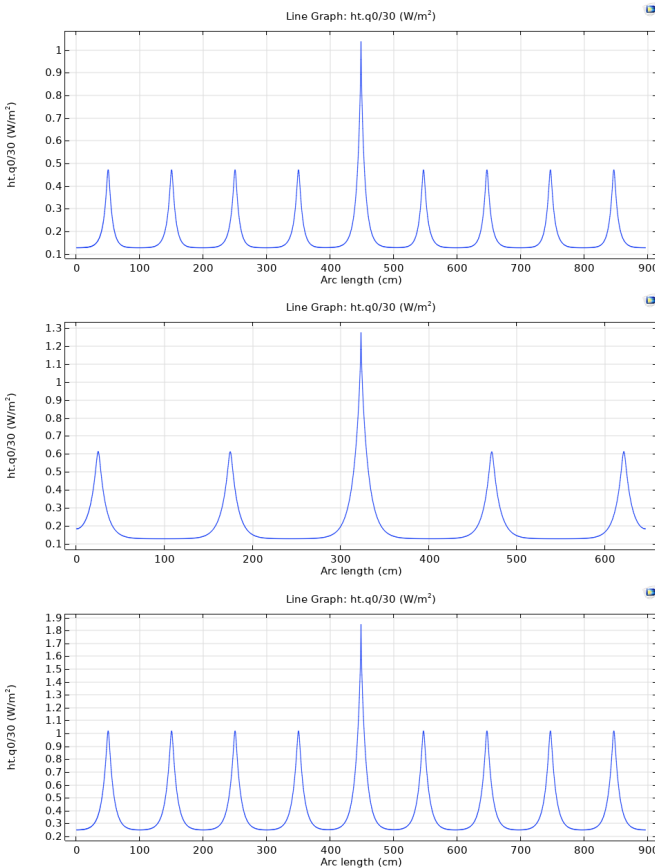


Figure 5. Temperature distribution for the assemblies W100-30-0.1 (top), W150-30-0.2 (middle), and W100-15-0.2 (bottom) with stainless steel.

capacity, density, water vapor resistance factor, and moisture isotherm. These were determined according to the ISO 14056:2007 standard (International Organization for Standardization, 2007).

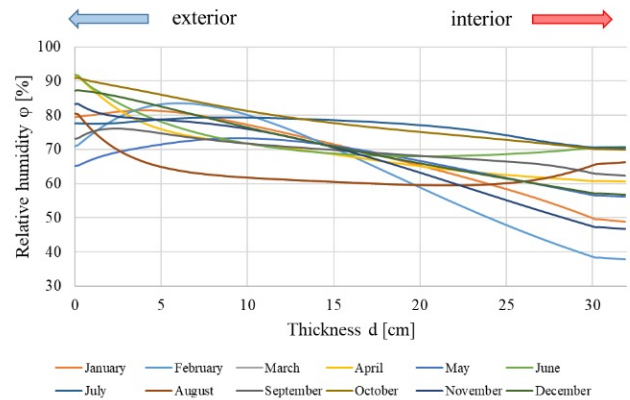


Figure 6. Distribution of the relative humidity over the wall cross section at the first day of each month.

Figure 6 shows the distribution of relative humidity computed across the cross section at the center of a wall element at the first day of each month. The relative humidity has a tendency to decrease towards the interior of the building. This is caused by diffusion that is mostly transporting humidity from inside to outside, because the indoor temperature exceeds the outdoor temperature for most of the time. The distribution of the humidity in the cross-section does not indicate humidity levels that might lead to excessive condensation. However, humidity levels around 90% are detected on the interior surface of the outside metal sheet. This is natural since the steel sheet cannot absorb moisture.

To investigate this phenomenon in more detail, we show in Figure 7 the temperature and relative humidity on the inner surface of outer metal sheet during one full year. The relative humidity remains below 90 % for most of the time so that the risk of condensation seems to be relatively small.

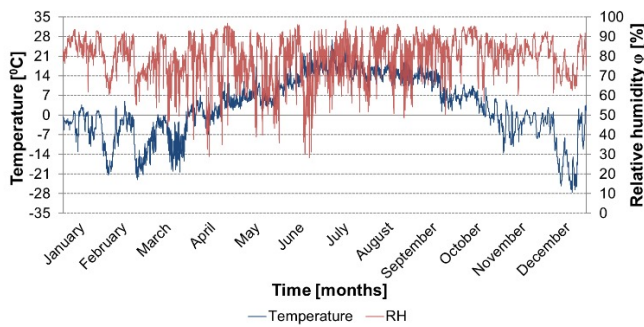


Figure 7. Temperature and relative humidity at the inner surface of the outside metal sheet during one year simulation.

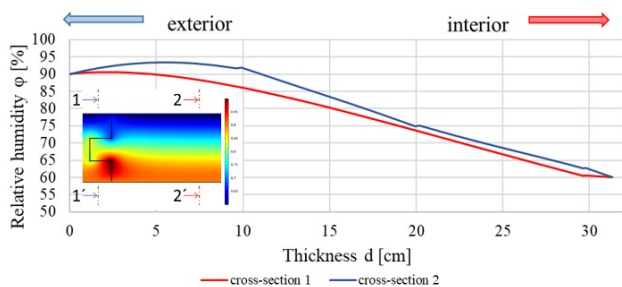


Figure 8. Relative humidity distribution in cross-section 1 (through joint between two elements) and cross-section 2 (through middle of an element).

A more detailed assessment of the hygrothermal performance of the wall was carried out by using a two-dimensional simulation model. In this case, a steady-state simulation was performed to detect whether there is a risk of excessive humidity at the joint between two elements. The boundary conditions were specified identically to the dynamic approach except that temperature and relative humidity which were set to 20°C and 50% for the inside and to 0°C and 90% for the outside, respectively.

As in the dynamic 1D case, the relative humidity does not seem to reach condensation levels under the defined conditions. However, as Figure 8 shows, higher relative humidity is found at the joint between two elements near the indoor wall. One possible reason for the humidity accumulation is the contact of permeable thermal insulation and the metal sheet. However, because the high level of relative humidity (>90%) is located near the indoor and the temperature should never drop below the freezing point there, the risk of freezing will remain small at this location.

5 Concluding Remarks

Cold-formed steel members in the building envelope can form thermal bridges that may affect the overall hygrothermal performance of the building quite considerably. We have introduced and studied a family of hollow cold-formed steel panels filled with insulation and parametrized with respect to their main structural dimen-

sions. Thermal performance of six unique panel geometries was examined computationally by using the COMSOL software while keeping the insulation properties fixed. The heat transfer analysis was based on well-established 2D steady state finite element analysis with typical boundary conditions.

The thermal analysis revealed a clear correlation between the thickness of the hollow section and the thermal bridging at the panel intersections. On the other hand, it is more difficult to assess fairly the influence of the panel thickness, width and depth to thermal bridging at building corners because the overall performance is influenced by the internal thermal bridges. We also showed that the notable difference between the thermal conductivities of stainless and mild steels is clearly reflected in the thermal performance of the corresponding wall assemblies.

We also performed time-dependent and steady-state hygrothermal analyses of the panels based on recent meteorological data from Oulu, Finland. The results showed that the hygrothermal conditions inside the studied elements do not give rise to a significant risk for excessive humidity and/or water condensation. However, it is of high importance to avoid any surface condensation on the interior surface of the wall, especially in the vicinity of thermal bridges e.g. by providing well-ventilated indoor environment and/or by adding thermal insulation on the exterior side of the wall assembly.

Our work provides the foundations for a further parametric optimization study of the structural elements where also local and global buckling phenomena of the thin sheets are considered. Further optimization of thermal and hygrothermal performance can also be carried out by refining the parametric space and developing novel optimization algorithms.

Acknowledgements

This research has been supported by the Kolartec-CBC project KO1089 Green Arctic Building. This support is gratefully acknowledged.

References

- Dan Dubina, Viorel Ungureanu, and Raffaele Landolfo. *Design of Cold-formed Steel Structures: Eurocode 3: Design of Steel Structures. Part 1-3 – Design of Cold-formed Steel Structures*. ECCS – European Convention for Constructional Steelwork, 2012.
- Gregory J Hancock, Thomas Murray, and Duane S Ellifrit. *Cold-formed Steel Structures to the AISI Specification*. CRC Press, 2001.
- D.J. Hopkin, J. El-Rimawi, V. Silberschmidt, and T. Lennon. An effective thermal property framework for softwood in parametric design fires: Comparison of the Eurocode 5 parametric charring approach and advanced calculation models. *Construction and Building Materials*, 25(5):2584–2595, 2011. doi:10.1016/j.conbuildmat.2010.12.002.

International Organization for Standardization. *ISO10456:2007 Building materials and products – Hygrothermal properties – Tabulated design values and procedures for determining declared and design thermal values*. International Organization for Standardization, 2007.

Divyansh R. Kapoor and Kara D. Peterman. Quantification and prediction of the thermal performance of cold-formed steel wall assemblies. *Structures*, 30:305–315, 2021. doi:10.1016/j.istruc.2020.12.060.

Eduardo Roque and Paulo Santos. The effectiveness of thermal insulation in lightweight steel-framed walls with respect to its position. *Buildings*, 7(1):13, 2017. doi:10.3390/buildings7010013.

Eduardo Roque, Rui Oliveira, Ricardo M.S.F. Almeida, Romeu Vicente, and Antonio Figueiredo. Lightweight and prefabricated construction as a path to energy efficient buildings: thermal design and execution challenges. *International Journal of Environment and Sustainable Development*, 19(1):1–32, 2020. doi:10.1504/IJESD.2020.105465.

N. Soares, P. Santos, H. Gervásio, J.J. Costa, and L. Simões Da Silva. Energy efficiency and thermal performance of lightweight steel-framed (LSF) construction: A review. *Renewable and Sustainable Energy Reviews*, 78:194–209, 2017. doi:10.1016/j.rser.2017.04.066.

Suomen Rakennusinsinöörien Liitto RIL ry. *RIL 107-2012 Rakennusten veden- ja kosteudeneristysohje (in Finnish)*. Suomen Rakennusinsinöörien Liitto RIL ry, 2012.